



ACADEMIC
PRESS

Available online at www.sciencedirect.com

SCIENCE @ DIRECT®

Journal of Solid State Chemistry 172 (2003) 138–147

JOURNAL OF
SOLID STATE
CHEMISTRY

<http://elsevier.com/locate/jssc>

Facile synthesis of interstitial metal nitrides with the filled β -manganese structure

Timothy J. Prior and Peter D. Battle*

Inorganic Chemistry Laboratory, University of Oxford, South Parks Road, Oxford OX1 3QR, UK

Received 17 September 2002; received in revised form 5 November 2002; accepted 18 November 2002

Abstract

A new family of nitrides, $\text{Ni}_{2-x}\text{M}'_x\text{Mo}_3\text{N}$ ($\text{M}' = \text{Co}$ or Pd ; $0 \leq x \leq 1.5$), has been prepared pure by nitridation of commercially available crystalline metal oxides under reducing conditions (10% H_2 in N_2). The simple synthesis employs standard solid-state techniques and does not require the preparation of reactive precursors. Substitution of Ni by Co or Pd leads to a linear increase of the unit cell volume with composition. The temperature, composition, and magnetic-field dependence of the molar magnetisation suggest that the introduction of Co, but not Pd, increases the degree of electron localisation in $\text{Ni}_{2-x}\text{M}'_x\text{Mo}_3\text{N}$. The same synthetic method has also led to the formation, in mixtures, of the new phases $\pi\text{-Co}_2\text{Mo}_3\text{N}$ and Pd_2N .

© 2003 Elsevier Science (USA). All rights reserved.

Keywords: Interstitial nitride; Beta-manganese structure; Nitride synthesis; Nitride magnetism

1. Introduction

Metal nitrides have attracted considerable attention due to a number of interesting properties which they display, for example hardness, [1,2] electrical [3,4] or thermal [5] conductivity, superconductivity, [6] magnetism, [7] and catalytic activity. [8,9] However, compared with the enormous range of ternary and higher metal oxides which is known, there is a dearth of mixed metal nitrides. There are a number of reasons for this, not least the refractory (and hence unreactive) nature of many binary nitrides and the extreme strength of the bond in dinitrogen. Elder et al. [10] have provided a means of predicting which ternary nitrides might be accessible. This is valuable when the appropriate thermodynamic data are available, but in general it is impossible to predict a priori whether a particular nitride will be stable.

The synthesis of binary nitrides is normally accomplished by one of two methods: reaction of the metal with nitrogen, often using a liquid metal flux, [11,12] or reaction of the metal oxide with ammonia. Synthesis of

ternary nitrides has been attempted by a number of routes. The majority of known ternary nitrides have been synthesised from binary nitrides and metals or by the ammoniation of ternary oxides. Other routes that have been utilised include ammoniation of metal sulphides [13] or amorphous mixed metal precursors. [14] Frequently the preparation of these precursors requires air-sensitive [14] or complex handling techniques (e.g., freeze-drying [15]) while the purity of products is often doubtful when ammonia is employed; binary metal nitrides, [14] alloys, [16] or pure metals [17] being common impurities. It is notable that there is no simple, generally applicable method for the formation of pure ternary metal nitrides.

The incorporation of non-metals in interstitial sites within metals and alloys leads to materials with increased hardness. This is believed to be due to strengthening of the metal–metal bonding. [2] One structure type adopted by a number of interstitial mixed metal compounds (borides, carbides, nitrides) which has been receiving interest is the filled β -Mn structure (sometimes denoted π -phase), M_2T_3X , which is exemplified by $\text{Al}_2\text{Mo}_3\text{C}$. [18,19] M atoms lie on the $8c$ positions of a cubic unit cell with space group symmetry $P4_132$ forming a single (10,3)-a network. [20] The space

*Corresponding author. Fax: +44-1865-272690.

E-mail address: peter.battle@chem.ox.ac.uk (P.D. Battle).

within this network is filled by corner-sharing T_6X octahedra. (Fig. 1) The structure is entirely analogous to that of β -Mn, differing only by the addition of the interstitial non-metal atoms.

Our attempts to synthesise nickel molybdenum oxides under conditions suitable for the formation of Mo^{IV} (standard ceramic synthesis techniques under flowing 10% hydrogen in nitrogen) did not yield the desired product; instead a mixture containing the β -Mn interstitial nitride $\text{Ni}_2\text{Mo}_3\text{N}$ was formed. Further experimentation showed that pure $\text{Ni}_2\text{Mo}_3\text{N}$ can be deliberately prepared in a simple procedure in which intimately ground crystalline metal oxides are heated under flowing synthesis gas (10% H_2 in N_2) and that the same method can be used to prepare the π -phase solid solutions $\text{Ni}_{2-x}\text{Co}_x\text{Mo}_3\text{N}$ and $\text{Ni}_{2-x}\text{Pd}_x\text{Mo}_3\text{N}$. During the course of these syntheses we were able to show that our protocol also simplifies the preparation of the η -phases $M_3\text{Mo}_3\text{N}$ ($M = \text{Fe}, \text{Co}$) [16] and leads to the formation of a new phase, tentatively identified as Pd_2N . We describe below the synthesis and structural characterisation of these phases and a preliminary survey of their magnetic properties.

2. Experimental

Reagents purities: Cobalt oxide (Johnson Matthey, 99.9985%), Iron oxide (Alfa Aesar, 99.998%), Nickel oxide (Johnson Matthey, 99.998%), Molybdenum dioxide (Alfa Aesar, 99%), Molybdenum trioxide (Alfa Aesar, 99.9995%), Palladium oxide (Johnson Matthey, 99.9%). Synthesis gas: 10% H_2 in N_2 (Air Products).

2.1. Synthesis of π -phases

$\text{Ni}_2\text{Mo}_3\text{N}$: (1) A stoichiometric mixture of NiO and MoO_3 was intimately ground and fired under flowing synthesis gas, for 72 h at 775°C and 24 h at 1000°C, with intermittent regrinding. (2) A stoichiometric mixture of NiO and MoO_2 was intimately ground and fired under flowing synthesis gas, for 48 h at 800°C and 24 h at 900°C and 1000°C, with intermittent regrinding.

Cobalt-doped phases: Stoichiometric mixtures of NiO, Co_3O_4 , and MoO_3 were intimately ground and fired under flowing synthesis gas for 48 h at 700°C, 750°C, 1000°C, and 1100°C, with intermittent regrinding.

Palladium-doped phases: Stoichiometric mixtures of NiO, PdO, and MoO_3 were intimately ground and fired under flowing synthesis gas, for 48 h at 700, 750, and twice at 1100°C, with intermittent regrinding.

2.2. Synthesis of η -phases

Stoichiometric mixtures of MoO_3 and either Co_3O_4 or Fe_2O_3 were intimately ground and fired under flowing synthesis gas, for 48 h at 700, and 24 h each at 750°C, 1000°C, and 1100°C, with intermittent regrinding.

In all cases samples were cooled to room temperature under flowing gas after switching off the furnace. No study of the effects of variation of the cooling rate was carried out. No special handling techniques were applied to samples following their removal from the furnace.

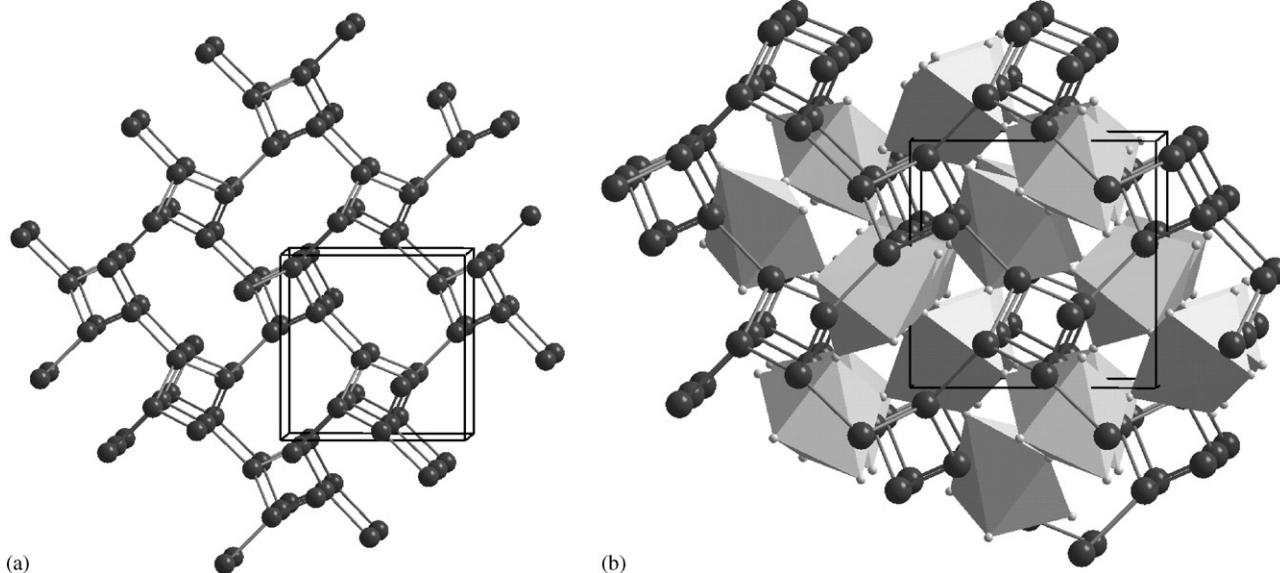


Fig. 1. Filled β -Mn structure of $\text{Ni}_2\text{Mo}_3\text{N}$. (a) Single (10,3)-a network of nickel atoms. (b) Nickel network (black spheres) filled with corner-sharing Mo_6N octahedra (grey).

2.3. Characterisation

The progress of synthesis was charted by X-ray powder diffraction using a Philips diffractometer operating with $\text{CuK}\alpha_1$ and $\text{K}\alpha_2$ radiation. Relatively high-resolution data to be used in quantitative analyses were collected using a Siemens D5000 diffractometer nominally operating with $\text{CuK}\alpha_1$ radiation over the angular range $10 \leq 2\theta / ^\circ \leq 125$ with a step size of 0.02° . However, imperfect monochromation introduced a contribution of approximately 2% $\text{K}\alpha_2$ which was allowed for in the data analysis. Rietveld refinement [21] of the crystal structures was carried out using the GSAS [22] suite of programs. Backgrounds were fitted using a shifted Chebyshev polynomial of the first kind. Peaks shapes were modelled using a pseudo-Voigt function.

TGA was performed using a Rheometric Scientific STA1500 instrument. Samples were loaded into platinum or alumina pans and heated under a flow (30 ml min^{-1}) of pure oxygen. Metal analysis was effected by ICP emission spectroscopy using a Thermo Jarell Ash Atomscan 16 spectrometer. Nitrogen analysis was performed using a Carlo Erber 1106 CHN analyser.

Magnetic measurements were carried out using a Quantum Design MPMS 5000 SQUID magnetometer. The sample magnetisation (M) was measured as a function of temperature ($5 \leq T/\text{K} \leq 350$) during warm up after cooling to 5 K in either zero field (ZFC) or in the measuring field of 100 Oe (FC). In selected cases, the

magnetisation was measured as a function of field ($-50 \leq H/\text{kOe} \leq 50$) after cooling to the measuring temperature in a field of 50 kOe. Attempts were made to fit the measured magnetic susceptibility (defined as $\chi = M/H$) to a Curie–Weiss law, modified to include a temperature-independent term. However, this function proved inadequate in many cases, and the discussion of the magnetic properties given below is largely qualitative.

3. Synthesis and structural chemistry

3.1. $\text{Ni}_2\text{Mo}_3\text{N}$

Rietveld analysis of X-ray powder diffraction data (Fig. 2) showed that $\text{Ni}_2\text{Mo}_3\text{N}$ crystallises with the filled β -Mn structure in the isomorphous pair of space groups $P4_132$ and $P4_332$. Crystal data are summarised in Table 1. It contains a net of nickel atoms, the holes in which are filled by Mo_6N octahedra. Within the net, the distance between neighbouring nickel atoms ($2.4694(6) \text{ \AA}$, 3-coordinate nickel) is similar to that for the pure metal ($2.492(1) \text{ \AA}$, 12-coordinate). The current synthesis of $\text{Ni}_2\text{Mo}_3\text{N}$ affirms the structural description of Herle et al. [17] although in contrast to their preparation which involved ammoniation of amorphous precursors prepared under air sensitive conditions, our X-ray diffraction patterns showed no evidence for the

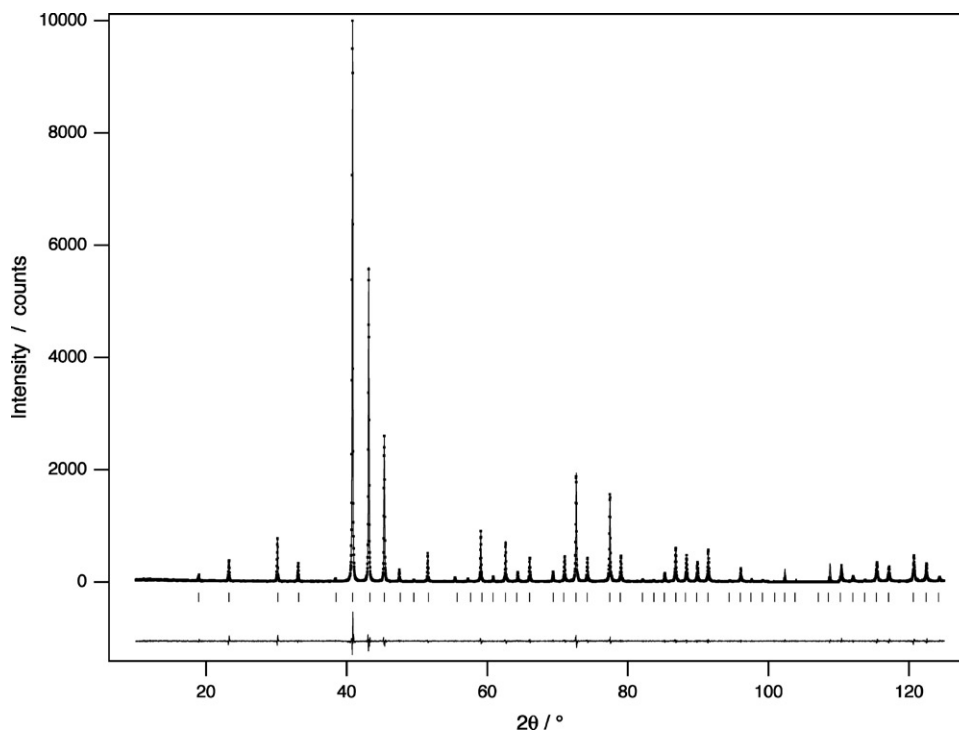


Fig. 2. Observed (\cdot), calculated ($-$), and difference X-ray powder diffraction profiles for $\text{Ni}_2\text{Mo}_3\text{N}$ at room temperature; tick marks indicate positions of allowed reflections from the $\text{K}\alpha_1$ diffraction. The final structural refinement converged with $R_{\text{wp}} = 0.1218$.

presence of molybdenum nitride (Mo_2N) in the final product.

The X-ray powder diffraction pattern of the TGA oxidation product showed the presence of only NiMoO_4 and MoO_3 . The increase in mass upon complete oxidation of $\text{Ni}_2\text{Mo}_3\text{N}$ to NiMoO_4 and MoO_3 is in good agreement with the calculated value: Calc. 38.6%, Found 37(1)%. Satisfactory chemical analysis data were obtained for $\text{Ni}_2\text{Mo}_3\text{N}$: Calc. % Ni 27.99, Mo 68.65, N 3.34, Found % Ni 27.94, Mo 68.65, N 3.20 (gives $\text{Ni}_2\text{Mo}_3\text{N}_{0.96}$).

Ex situ X-ray powder diffraction data charting the course of reaction gave an insight into the mechanism

of formation of the compound. Following the initial heating at 700°C , X-ray powder diffraction patterns showed the presence of MoO_2 , NiO , and the desired product. This suggests that prior to the formation of the final product, a stepwise reduction of molybdenum trioxide is occurring. Synthesis employing a stoichiometric mixture of MoO_2 and NiO under H_2/N_2 also lead to the formation of $\text{Ni}_2\text{Mo}_3\text{N}$, although this is less convenient as it is rather difficult to obtain the starting material MoO_2 highly pure.

3.2. $\text{Ni}_{2-x}\text{Co}_x\text{Mo}_3\text{N}$ ($x = 0.5, 0.75, 1, \text{ and } 1.5$)

Compounds in the solid solution obtained by substitution of Ni by Co may be synthesised using the same protocol. The initial cobalt source (Co_3O_4) is more difficult to reduce than the nickel oxide, therefore a number of firings at 1100°C were necessary.

Rietveld analyses of X-ray patterns (Fig. 3) showed that these compounds are isostructural with the parent phase $\text{Ni}_2\text{Mo}_3\text{N}$, displaying a smooth increase in cubic unit cell parameter with increasing cobalt content, consistent with the larger size of cobalt. (Fig. 4) It is not possible to determine by X-ray diffraction whether there is any ordering of the nickel and cobalt within the structure and these two elements were, therefore, assumed to be disordered over the $8c$ sites. There is no

Table 1
Atomic positions for filled β -manganese nitrides $\text{Ni}_2\text{Mo}_3\text{N}$ and $\text{Co}_2\text{Mo}_3\text{N}$

Atom	Wyckoff position	x	y	z	$U_{\text{iso}}/\text{\AA}^2$
$\text{Ni}_2\text{Mo}_3\text{N}$ Space group $P4_132$, $a_0 = 6.63582(3) \text{\AA}$, $R_{\text{wp}} = 0.1218$					
Ni	$8c$	0.0670(1)	0.0670(1)	0.0670(1)	0.0108(9)
Mo	$12d$	1/8	0.20153(6)	0.45153(6)	0.0086(7)
N	$4a$	3/8	3/8	3/8	0.012(3)
$\text{Co}_2\text{Mo}_3\text{N}$ Space group $P4_132$, $a_0 = 6.6653(1) \text{\AA}$, $R_{\text{wp}} = 0.0425$					
Co	$8c$	0.0671(3)	0.0671(3)	0.0671(3)	0
Mo	$12d$	1/8	0.2024(2)	0.4524(2)	0.06(3)
N	$4a$	3/8	3/8	3/8	0

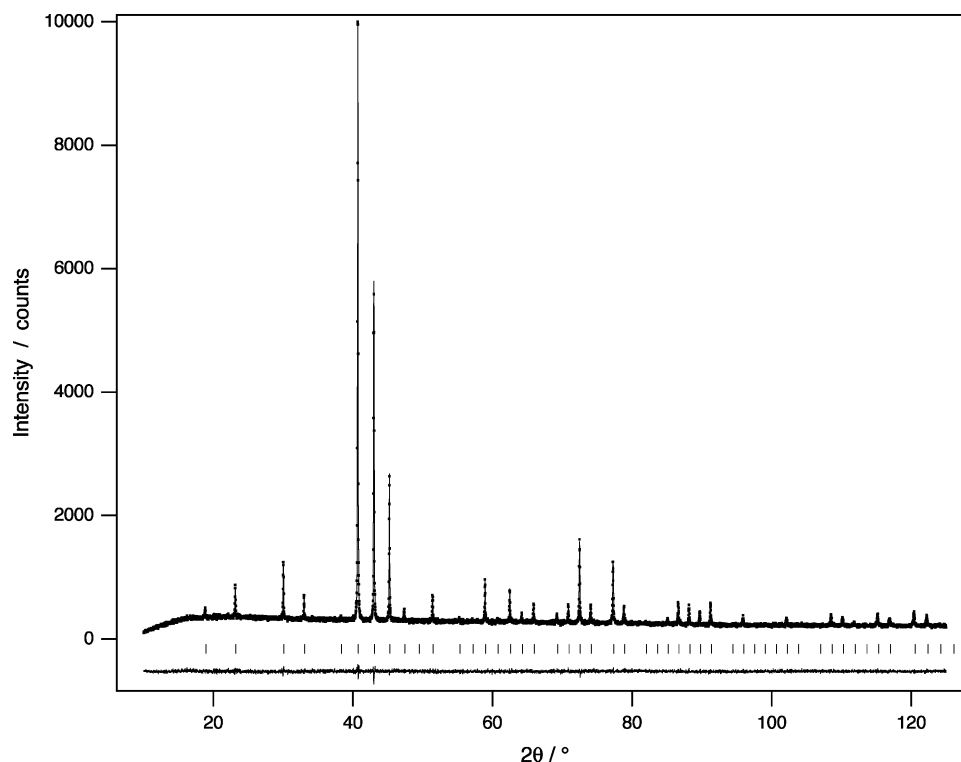


Fig. 3. Observed (\cdot), calculated ($-$), and difference X-ray powder diffraction profiles for NiCoMo_3N at room temperature; tick marks indicate positions of allowed reflections from the $K\alpha_1$ diffraction. The final structural refinement converged with $R_{\text{wp}} = 0.051$.

evidence however to suggest the incorporation of the first row transition metals into the Mo_6N octahedra. Satisfactory TGA oxidation analyses were obtained for all compositions within the series, indicating full nitrogen occupancy and ideal metal stoichiometry. These are detailed in Table 2. Chemical analysis of the nitrogen content for one representative composition, NiCoMo_3N , was consistent with the expected analysis: Calc. % N 3.34, Found % N 3.37. For $\text{Ni}_{0.5}\text{Co}_{1.5}\text{Mo}_3\text{N}$, peaks corresponding molybdenum metal (2.7(1)% by weight) and to the known phase $\text{Co}_3\text{Mo}_3\text{N}$ [16] (2.1(2)% by weight) were present in the X-ray diffraction pattern.

3.3. $\text{Co}_2\text{Mo}_3\text{N}$

It proved possible to synthesise this previously unknown phase, albeit not in a pure form, by reduction under nitriding conditions. Previous attempts to synthesise this phase by plasma nitridation of oxides or via air-sensitive precursors have yielded only the η -phase $\text{Co}_3\text{Mo}_3\text{N}$. [16] Indeed our studies also suggest that

the more cobalt-rich phase is preferred: reduction-nitridation of a 1:1 stoichiometric mixture of cobalt and molybdenum oxides yielded a pure sample of $\text{Co}_3\text{Mo}_3\text{N}$. Before the final firing small amounts of Co_3O_4 , MoO_2 and $\text{Co}_2\text{Mo}_3\text{N}$ were present, but these reacted to give the desired product.

$\text{Co}_2\text{Mo}_3\text{N}$ again crystallises with the filled β -Mn structure. (Table 1) However, X-ray powder diffraction studies of this reaction product (Fig. 5) showed the

Table 2
Ratio of initial and final mass of $\text{Ni}_{2-x}\text{M}_x\text{Mo}_3\text{N}$ ($M = \text{Co}, \text{Pd}$) upon complete oxidation under flowing oxygen

$\text{Ni}_{2-x}\text{M}_x\text{Mo}_3\text{N}$		x				
		0.5	0.75	1	1.5	2
$M = \text{Co}$	Calculated	1.31	1.31	1.31	1.31	1.31
	Observed	1.33	1.33	1.33	1.31	1.35
$M = \text{Pd}$	Calculated	1.37	1.36	1.35	1.33	1.31
	Observed	1.35	1.33	1.28	1.31	1.28

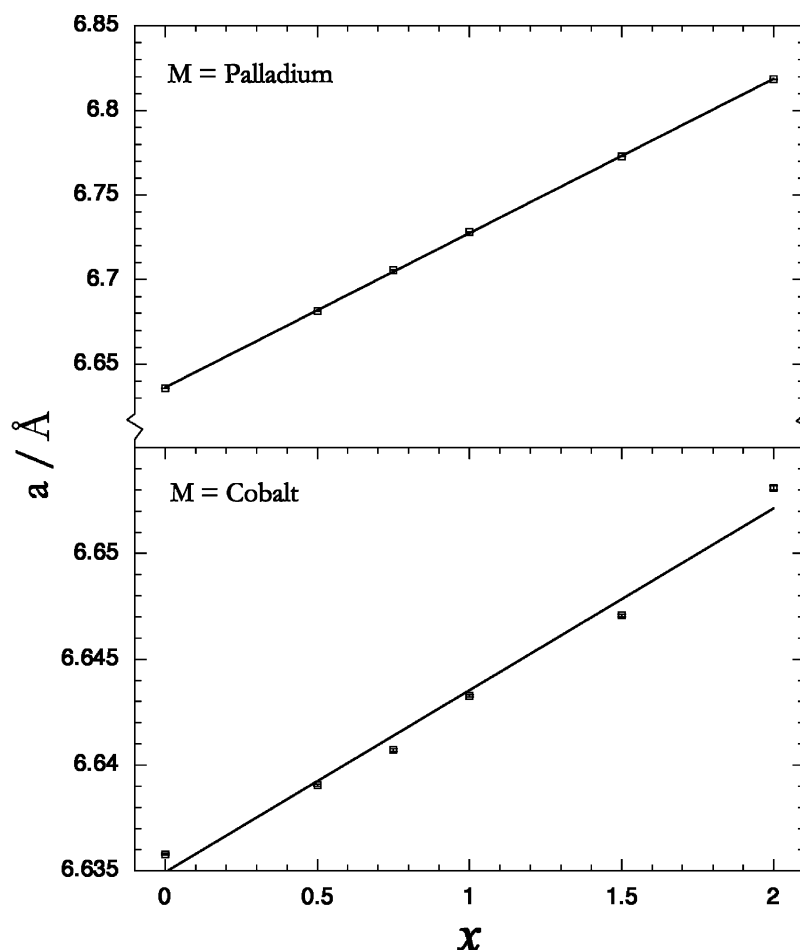


Fig. 4. Variation of unit cell parameter with composition for $\text{Ni}_{2-x}\text{M}_x\text{Mo}_3\text{N}$ ($M = \text{Co}, \text{Pd}$). Linear fits have been made through the data points. Error bars are contained within the points.

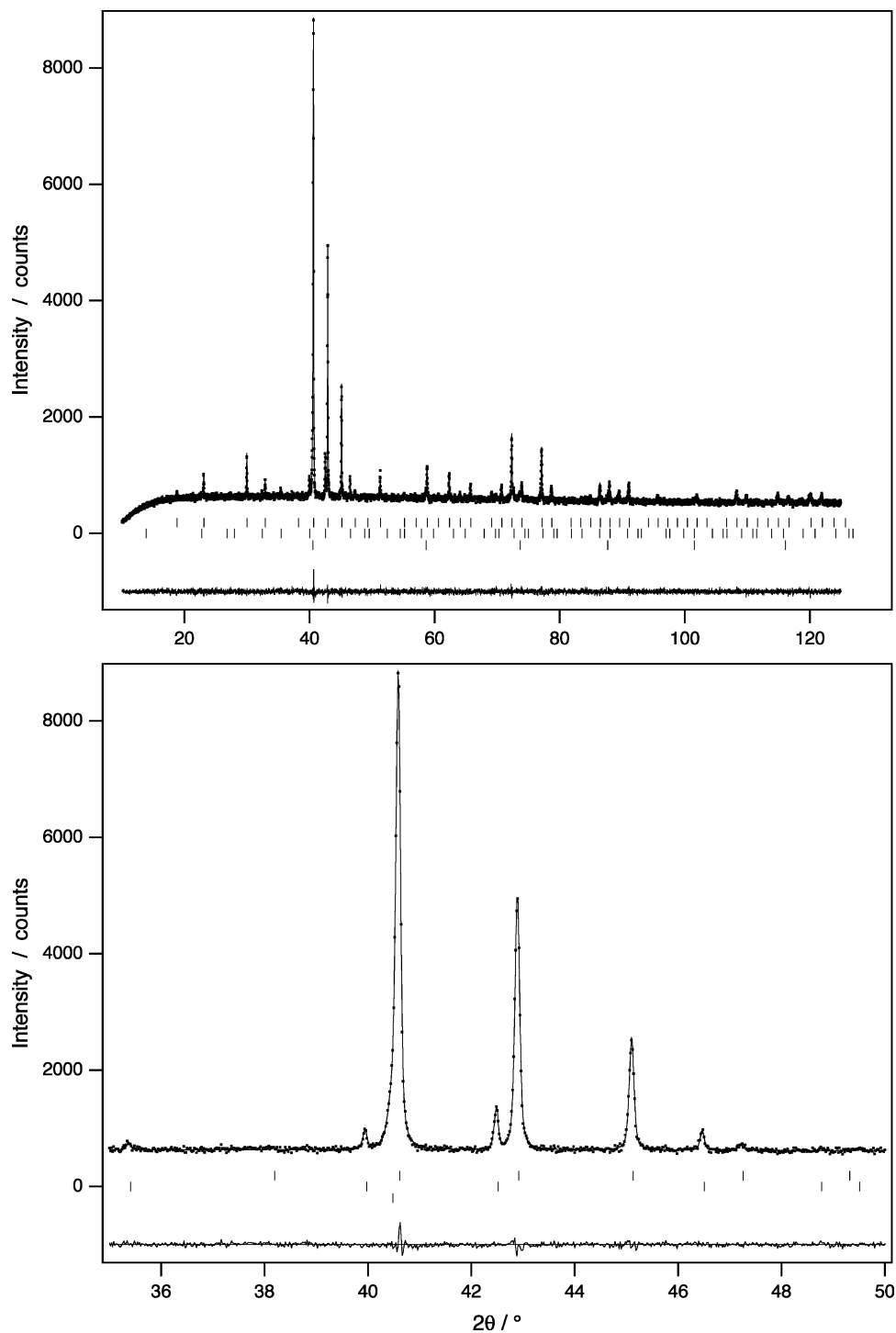


Fig. 5. Observed (\cdot), calculated ($-$), and difference X-ray powder diffraction profiles for $\text{Co}_2\text{Mo}_3\text{N}$ at room temperature; the top tick marks indicate positions of allowed reflections from the $K\alpha_1$ diffraction for $\text{Co}_2\text{Mo}_3\text{N}$, the middle marks correspond to $\text{Co}_3\text{Mo}_3\text{N}$, and the lowest are for Mo. The final structural refinement converged with $R_{\text{wp}} = 0.0425$.

presence of small amounts of molybdenum metal (4.8(3)% by weight) and $\text{Co}_3\text{Mo}_3\text{N}$ (7.7(3)% by weight). Upon prolonged heating the favoured products were $\text{Co}_3\text{Mo}_3\text{N}$ and molybdenum. We emphasise that no impurities were observed in $\text{Ni}_{2-x}\text{Co}_x\text{Mo}_3\text{N}$ over the composition range $0 \leq x \leq 1$.

3.4. $\text{Fe}_3\text{Mo}_3\text{N}$

This phase has been prepared previously in a pure form by a method involving ammoniation of amorphous oxide precursors. [16] The X-ray diffraction pattern (Fig. 6) of the product prepared by our simpler

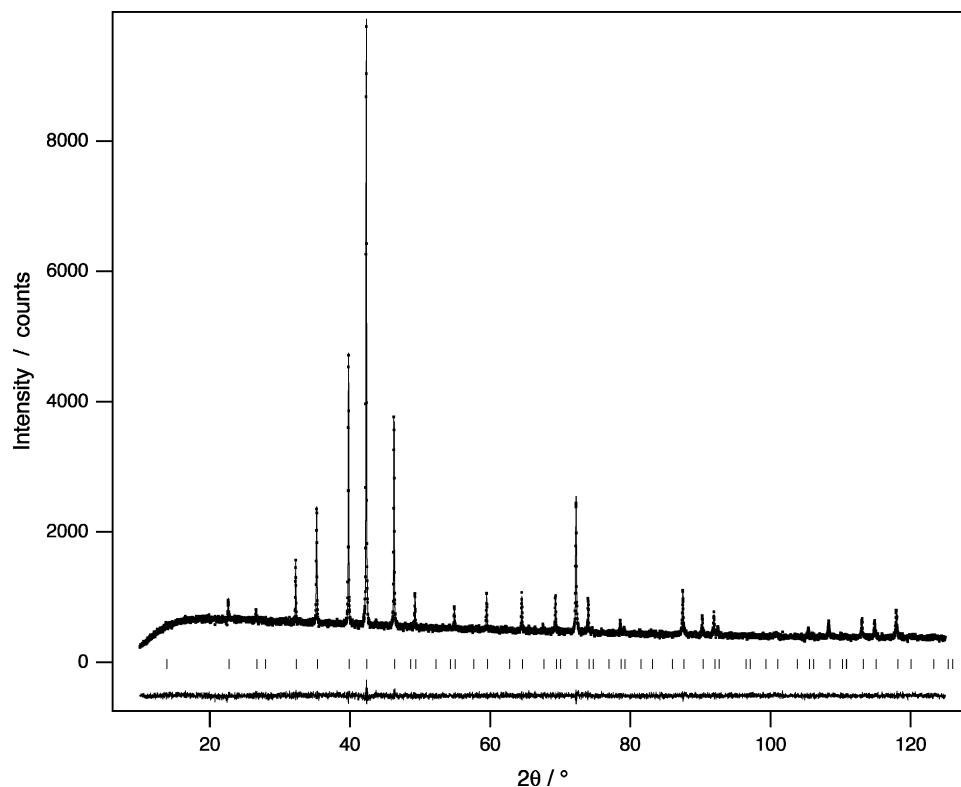


Fig. 6. Observed (\cdot), calculated ($-$), and difference X-ray powder diffraction profiles for $\text{Fe}_3\text{Mo}_3\text{N}$ at room temperature; tick marks indicate positions of allowed reflections from the $K\alpha_1$ diffraction. The final structural refinement converged with $R_{\text{wp}} = 0.0441$.

route is in excellent agreement with that reported previously ($a_0 = 11.0802(2) \text{ \AA}$).

3.5. $\text{Ni}_{2-x}\text{Pd}_x\text{Mo}_3\text{N}$ ($x = 0.5, 0.75, 1, 1.5, \text{ and } 2$)

Palladium may also be introduced into the network of transition metal atoms. Synthesis was accomplished in the same fashion. Rietveld refinement against X-ray diffraction data (Fig. 7) shows that all of the compounds in this series crystallise with the filled β -Mn structure with no apparent ordering of Ni and Pd. Satisfactory TGA oxidation analyses were obtained for all compositions within the series. (Table 2) As the amount of palladium included is increased there is a smooth increase in the lattice parameter, as shown in Fig. 4. No impurity phases were detected for $0 \leq x \leq 1.5$, but the X-ray powder diffraction pattern of the known $\text{Pd}_2\text{Mo}_3\text{N}$ [23] did contain weak peaks which could not be indexed using the cubic unit cell of the main phase. Attempts to fit the impurity peaks using a mixture of possible impurities, including Mo_2N and Pd, were unsatisfactory. Indexing of these peaks suggested the presence of a phase with a small orthorhombic unit cell, similar to that of Co_2N . A significant improvement was made to the fit when 2.29(9)% by weight of a phase with the Co_2N structure and composition Pd_2N was

included in the data analysis. (Table 3) This phase has not been reported previously.

4. Magnetism

Measurements of magnetisation as a function of temperature for $\text{Ni}_2\text{Mo}_3\text{N}$ showed that the compound is weakly Pauli paramagnetic. Consistent magnetic behaviour was displayed across a number of samples, in contrast to the variation in behaviour previously reported. [17] We ascribe this to the absence of impurities in our samples. The low magnetic susceptibility (Fig. 8a) is consistent with the Pauli paramagnetism expected of a delocalised electron system, although the Curie-like component and the small hysteresis observed at low temperatures show that this cannot be a complete description of this compound. The replacement of 25% Ni by Co causes a marked increase in both the susceptibility (Fig. 8b) and the level of hysteresis; the data plotted in Fig. 9 show a remanent magnetisation of $2.72 \times 10^{-4} \mu_{\text{B}}$ per formula unit at 5 K. The susceptibility (Fig. 8c) of the 50%—substituted composition NiCoMo_3N shows a relatively rapid increase at $\sim 80 \text{ K}$, with a remanent magnetisation of $2.66 \times 10^{-4} \mu_{\text{B}}$ per formula unit at 5 K. However, the susceptibility (Fig. 8d) of $\text{Ni}_{0.5}\text{Co}_{1.5}\text{Mo}_3\text{N}$, although comparable in

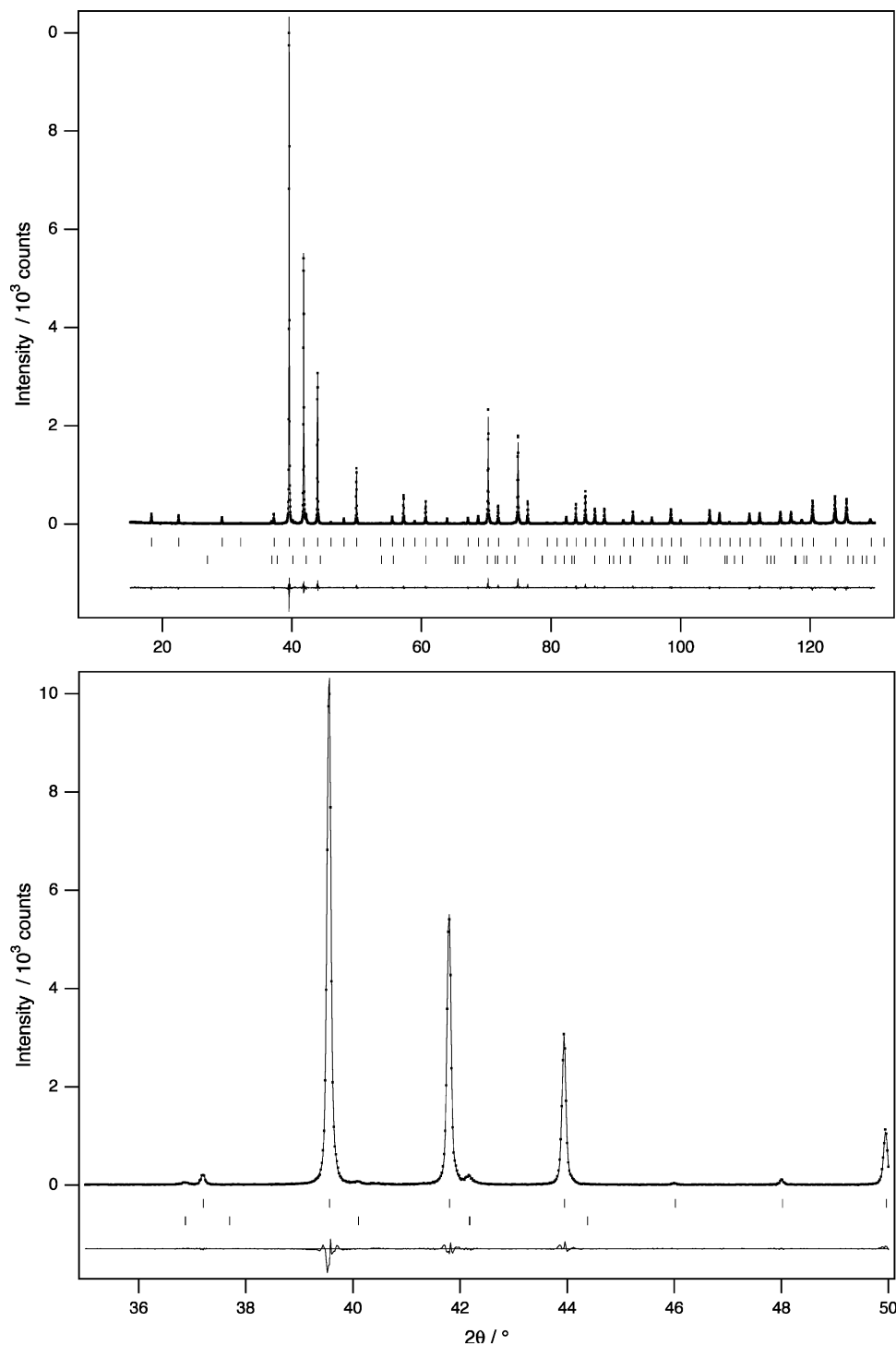


Fig. 7. Observed (\cdot), calculated ($-$), and difference X-ray powder diffraction profiles for $\text{Pd}_2\text{Mo}_3\text{N}$ at room temperature; upper tick marks indicate positions of allowed reflections from the $K\alpha_1$ diffraction for $\text{Pd}_2\text{Mo}_3\text{N}$ and the lower set correspond to Pd_2N . The final structural refinement converged with $R_{\text{wp}} = 0.1375$.

magnitude to that of NiCoMo_3N , shows less hysteresis. In contrast, the introduction of Pd causes only a small change in susceptibility and relatively little hysteresis (Fig. 8e). The two chosen substituents, Co and Pd, come respectively from the first ($3d$) and second ($4d$)

transition series. Energy bands formed from the $3d$ orbitals of the former will be comparable in width to those involving $3d$ Ni orbitals and narrower than those which have a large contribution from the $4d$ orbitals of Pd. The disorder on the transition metal sublattice in the

Table 3
Atomic positions for Pd₂N with the Co₂N structure

Atom	Wyckoff position	x	y	z
N	2a	0	0	0
Pd	4g	0	0.351(4)	0.242(5)
Space group		<i>Pmmn</i> (no. 58)		
<i>a</i> /Å		2.808(1)		
<i>b</i> /Å		4.863(2)		
<i>c</i> /Å		4.4869(9)		

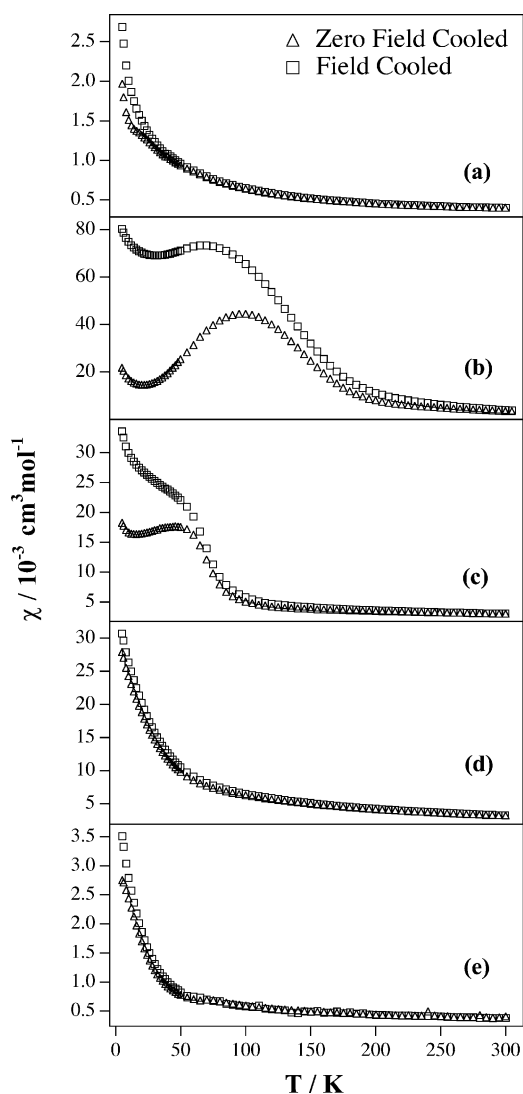


Fig. 8. Variation of molar magnetic susceptibility with temperature for: (a) Ni₂Mo₃N, (b) Ni_{1.5}Co_{0.5}Mo₃N, (c) NiCoMo₃N, (d) Ni_{0.5}Co_{1.5}Mo₃N and (e) Ni_{1.5}Pd_{0.5}Mo₃N.

substituted compositions will favour localisation of the *d* electrons, as will the relatively narrow energy width of the *3d* bands. Our observations can thus be explained by assuming that the disorder introduced by Co-doping

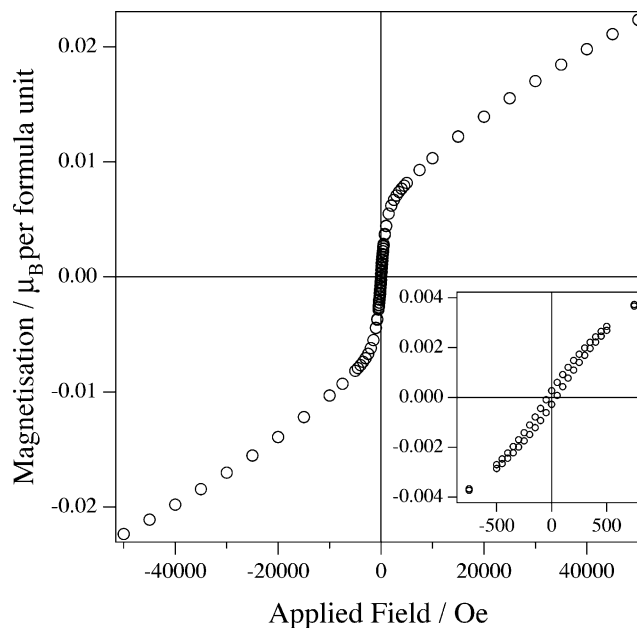


Fig. 9. Magnetisation of Ni_{1.5}Co_{0.5}Mo₃N as a function of applied field at 5 K.

causes partial electron localisation and therefore an increase in the magnetic susceptibility, whereas the *4d* levels of Pd are sufficiently broad to overcome this effect. However, the replacement of Ni by Co (but not Pd) changes the number of electrons in the system, and this factor will also have to be taken into account in producing a more comprehensive account of the magnetic behaviour.

5. Conclusion

The principal purpose of this publication is to demonstrate that the solid-state synthesis of ternary, low-valent nitrides under reducing conditions can be a simple and clean procedure. We have prepared samples of the π -phase Ni₂Mo₃N with a higher level of purity than was obtained previously when more complex synthetic procedures were used. We have also used the method to prepare for the first time pure samples of the solid solutions Ni_{2-x}M'_xMo₃N (*M'* = Co, 0 ≤ *x* ≤ 1; *M'* = Pd, 0 ≤ *x* ≤ 1.5) and impure samples of Ni_{0.5}Co_{1.5}Mo₃N, π -Co₂Mo₃N and Pd₂N. We have also been able to prepare pure the known η -phases, Co₃Mo₃N and Fe₃Mo₃N. We hope that in the future the method will lead to the synthesis of many new nitrides with interesting properties.

Acknowledgments

We thank EPSRC for financial support.

References

- [1] L.E. Toth, in: *Transition Metal Carbides and Nitrides, Refractory Materials*, Vol. 7, Academic Press, New York, 1971.
- [2] S.T. Oyama, *The Chemistry of Transition Metal Carbides and Nitrides*, Blackie Academic and Professional, London, 1996.
- [3] S. Yoshida, *Proceedings of the 32nd IEEE Conference on Electrical Components* 1982, pp. 530–535.
- [4] R.M. Fix, R.G. Gordon, D.M. Hoffman, *Chem. Mater.* 2 (1990) 235–241.
- [5] K. Watari, *J. Ceram. Soc. Japan* 109 (2001) S7–S16.
- [6] F.H. Horn, W.T. Ziegler, *J. Am. Chem. Soc.* 69 (1947) 2762–2769.
- [7] J.M.D. Coey, H. Sun, *J. Magn. Magn. Mater.* 87 (1990) L251–L254.
- [8] C.J.H. Jacobsen, *Chem. Commun.* (2000) 1057–1058.
- [9] P.W. Lednor, *Catal. Today* 15 (1992) 177–337 (Complete issue).
- [10] S.H. Elder, F.J. DiSalvo, L. Torpor, A. Navrotsky, *Chem. Mater.* 5 (1993) 1545–1553.
- [11] F.J. DiSalvo, *Mater. Sci. Forum* 325–6 (2000) 3–10.
- [12] O. Reckeweg, J.C. Molstad, F.J. DiSalvo, *J. Alloy. Compd.* 315 (2001) 134–142.
- [13] F. Tessier, R. Marchand, Y. Laurent, *J. Eur. Ceram. Soc.* 17 (1997) 1825–1829.
- [14] K.S. Weil, P.N. Kumta, J. Grins, *J. Solid State Chem.* 146 (1999) 22–35.
- [15] S. Alconchel, F. Sapina, D. Beltran, A. Beltran, *J. Mater. Chem.* 9 (1999) 749–755.
- [16] S.K. Jackson, R.C. Layland, H.-C. zur Loye, *J. Alloy. Compd.* 291 (1999) 94–101.
- [17] P.S. Herle, M.S. Hegde, K. Sooryanarayana, T.N.G. Row, G.N. Subbanna, *Inorg. Chem.* 37 (1998) 4128–4130.
- [18] W. Jeitschko, H. Nowotny, F. Benesovsky, *Monatsh. Chem.* 95 (1964) 1212–1218.
- [19] W. Jeitschko, H. Nowotny, F. Benesovsky, *Monatsh. Chem.* 94 (1963) 247–251.
- [20] A.F. Wells, *Three-dimensional Nets and Polyhedra*, Wiley, New York, 1977.
- [21] H.M. Rietveld, *J. Appl. Cryst.* 2 (1969) 65–71.
- [22] A.C. Larson, R.B. von-Dreele, *General Structure Analysis System (GSAS)*, Los Alamos National Laboratories, 1990.
- [23] A. El-Himri, F. Sapina, R. Ibanez, A. Beltran, *J. Mater. Chem.* 11 (2001) 2311–2314.